Continental-Scale Partitioning of Fire Emissions During the 1997 to 2001 El Niño/La Niña Period

Guido R. van der Werf,[1]* James T. Randerson,[2]†
G. James Collatz,[3] Louis Giglio,[4] Prasad S. Kasibhatla,[5]
Avelino F. Arellano Jr.,[5] Seth C. Olsen,[2] Eric S. Kasischke[6]

During the 1997 to 1998 El Niño, drought conditions triggered widespread increases in fire activity, releasing CH_4 and CO_2 to the atmosphere. We evaluated the contribution of fires from different continents to variability in these greenhouse gases from 1997 to 2001, using satellite-based estimates of fire activity, biogeochemical modeling, and an inverse analysis of atmospheric CO anomalies. During the 1997 to 1998 El Niño, the fire emissions anomaly was 2.1 ± 0.8 petagrams of carbon, or 66 ± 24% of the CO_2 growth rate anomaly. The main contributors were Southeast Asia (60%), Central and South America (30%), and boreal regions of Eurasia and North America (10%).

Global atmospheric CO_2 and CH_4 levels are increasing, but at variable rates from year to year (*1*–*5*). Because both are greenhouse gases, our ability to predict future changes in climate depends, in part, on our understanding of the sources of this variation (*6*). Atmospheric CO_2 has been systematically measured since 1958, and during this time, the annual growth rate has ranged from nearly zero to roughly the rate at which fossil fuels were being combusted (*1*, *3*). A combination of atmospheric measurements (*3*), inverse modeling (*7*), and ocean observations and modeling (*8*) has attributed most of this variability to changes within the terrestrial biosphere.

Proposed mechanisms to explain the observed variability in CO_2 growth rate have focused primarily on the balance between terrestrial photosynthesis and ecosystem respiration (*7*, *9*–*11*). A recent study by Langenfelds *et al.* (*12*), however, provided evidence that parallel changes in atmospheric CO_2, CO, CH_4, and other trace gas species emitted by fires imply that a large part of the CO_2 variability in the 1990s was a result of variability in global fire emissions. This result is consistent with reports of increased fire activity during the 1997 to 1998 El Niño in Indonesia (*13*), Central America (*14*), parts of Amazonia (*15*, *16*), multiple countries in Africa (*14*), and boreal regions of North America and Eurasia (*17*, *18*). Although inverse studies have connected the fires in Indonesia and Southeast Asia with the spatial-temporal pattern of global atmospheric CO_2 anomalies during this period (*19*, *20*), a quantitative partitioning of global fire emissions among the continental regions has not yet been attempted. This information may provide insight into the biogeochemical and socioeconomic processes that regulate biosphere-atmosphere exchange of CO_2 and CH_4.

Here we present a means of isolating the contributions of fire emissions from different continents to atmospheric CO_2 and CH_4 concentration anomalies for the 5-year period from January 1997 through December 2001. This time period includes a strong El Niño (1997 to 1998) and a La Niña (1999 to 2000) (*21*). Our analysis consisted of two steps. First, we combined satellite observations of fire activity over this period from the Tropical Rainfall Measuring Mission–Visible and Infrared Spectrometer (TRMM-VIRS), European Remote Sensing Satellite–Along Track Scanning Radiometer (ERS-ATSR), and Terra MODerate resolution Imaging Spectroradiometer (Terra-MODIS) sensors with the Carnegie-Ames-Stanford Approach (CASA) biogeochemical model (*22*) to estimate interannual fire emissions at a 1° by 1° spatial resolution and with a monthly time step. We converted TRMM-VIRS (1998 to 2001) and ERS-ATSR (1997 to 2001) fire activity data to time series of burned area using MODIS burned area estimates (available for limited 10° by 10° areas starting in 2001) in the tropics, and using country-level burned-area statistics in the northern extratropics (*23*). The CASA model used this burned-area time series to estimate carbon emissions from fires, taking into account local variations in fuel type, fuel density, and combustion completeness (*22*, *23*). Carbon emissions from CASA were multiplied by biome-dependent emission factors (*24*) to obtain CO, CO_2, and CH_4 fire emissions (*25*). We then used the Goddard Earth Observing System Atmospheric Chemistry Transport Model (GEOS-CHEM) atmospheric chemistry transport model (*26*) to predict the temporal and spatial distribution of the emitted CO, CO_2, and CH_4 during the 1997 to 2001 period, separately tracking the unique space-time pattern of the emitted trace gases from seven continental-scale regions (listed in Table 1).

In the second step of our analysis, using a least squares inversion, we solved for the linear combination of the seven patterns of CO concentration anomalies generated from our forward model that minimized the difference with observed CO concentration anomalies at flask stations from the National Oceanic and Atmospheric Administration Climate Monitoring and Diagnostics Laboratory (NOAA/CMDL) (*27*). In this step, we assumed that fires caused all of the observed monthly anomalies of atmospheric CO from 1997 through 2001. In addition to fire emissions, other major sources of tropospheric CO include emissions from fossil fuel and biofuel combustion, CH_4 oxidation by OH, and oxidation of volatile organic compounds (*28*). Although these sources contribute substantially to mean latitudinal and seasonal variations of atmospheric CO (*28*), our assumption that these sources influenced the anomalies only minimally over the 1997 to 2001 period was predicated by the large variations in fire emissions during this period [e.g., (*27*)]. Because satellite and biogeochemical model information was used to construct the form of the basis function in each region, no additional a priori constraints were applied in the inversion. We assumed a 5 parts per billion (ppb) error for the monthly mean CO concentrations from each station on the basis of observed variations and measurement precisions (*27*). The seven scalars that we solved for in the inversion were then used to separately adjust the regional time series of carbon, CO_2, and CH_4 emissions that we obtained from our forward model (*23*).

Widespread increases in fire emissions occurred across multiple continents during the August 1997 to September 1998 period (Fig. 1A) and appeared to be linked in many regions with El Niño–induced drought (*29*). Over the entire 1997 to 2001 period, contributions to mean annual emissions were greatest from southern South America (23%), northern Africa (23%), and southern Africa (29%) (Fig. 1B and Table 1). Other important but smaller contributions came from Southeast Asia (10%), Central America and north-

[1]U.S. Department of Agriculture–Foreign Agricultural Service, National Aeronautics and Space Administration–Goddard Space Flight Center (NASA-GSFC), Code 923, Greenbelt Road, Greenbelt, MD 20771, USA. [2]Divisions of Geological and Planetary Sciences and Engineering and Applied Science, California Institute of Technology, Mail Stop 100-23, Pasadena, CA 91125, USA. [3]NASA-GSFC, Code 923, Greenbelt Road, Greenbelt, MD 20771, USA. [4]Science Systems and Applications, Inc., NASA-GSFC, Code 923, Greenbelt Road, Greenbelt, MD 20771, USA. [5]Nicholas School of the Environment and Earth Sciences, Duke University, Durham, NC 27708, USA. [6]Department of Geography, University of Maryland, College Park, MD 20742, USA.

*To whom correspondence should be addressed. E-mail: guido@ltpmailx.gsfc.nasa.gov
†Present address: Department of Earth System Science, University of California Irvine, 3212 Croul Hall, Irvine, CA 92697, USA.

ern South America (8%), the boreal region (4%), and other regions (4%) (Table 1). The calculated anomalies did not scale linearly with mean annual emissions; some regions with low average emissions (notably tropical and boreal forests) had high anomalies, including Southeast Asia in late 1997, Central and northern South America in early 1998, and northern boreal forests in mid-1998.

Observed atmospheric CO anomalies over the 1997 to 2001 period are shown in Fig. 2A. The largest positive anomalies occurred in regions north of 60°N during October of 1998 and were in excess of 70 ppb (*27*). Our forward biogeochemical and atmospheric modeling approach captured the timing and latitudinal distribution of the observed northern hemisphere CO anomalies but underestimated their magnitude (Fig. 2B). In addition, the forward modeling approach substantially underestimated positive CO anomalies between 30°N and 30°S in late 1997. In Fig. 2, C to E, we show examples of CO anomalies solely arising from variability in fire emissions from three important fire regions: boreal regions of North America and Eurasia, Central America and northern South America, and Southeast Asia. Inspection of the CO anomaly patterns from our forward model provided insight about several aspects of the relation between regional fire emissions and the distribution of atmospheric CO. Increased levels of fire emissions from boreal forests, for example, appeared to be largely responsible for the positive CO anomaly observed north of 30°N in late 1998. CO anomalies arising from tropical fires (Fig. 2, D and E) were almost an order of magnitude smaller than those from boreal fires at stations north of 30°N, and even if these signals were greatly amplified, they would not have had the correct space-time pattern to explain all of the northern CO anomalies. Another observation is that we underestimated the contribution of fire anomalies from Southeast Asia between 0° and 30°S in late 1997 (Fig. 2E).

A quantitative perspective on these features is provided by the atmospheric CO inversion; the least squares solution required higher CO emissions anomalies than predicted by our forward modeling approach during the August 1997 to September 1998 period from Southeast Asia (300 ± 62 Tg CO), Central America and northern South America (90 ± 40 Tg CO), northern boreal forests (57 ± 4 Tg CO), and southern South America (48 ± 23 Tg CO) (table S1). On a global basis, emissions anomalies from these four regions accounted for 95%

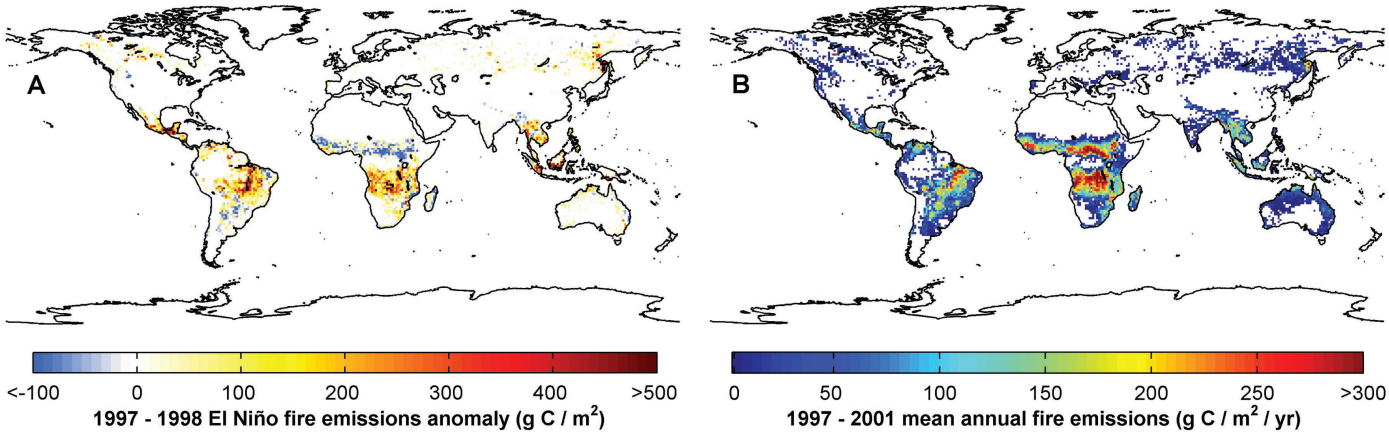

Fig. 1. (**A**) Emissions anomalies from fire during the August 1997 to September 1998 period (g C m^{-2}). This period had the highest emissions during 1997 to 2001 and is defined in the text as the El Niño period because it overlaps substantially with negative indices of the Southern Oscillation Index. Elevated emissions occurred across Central America, South America, southern Africa, Southeast Asia, Canada, and the Russian Far East. Emissions anomalies in each 1° by 1° grid cell were estimated with VIRS, ATSR, and MODIS satellite data and the CASA biogeochemical model. (**B**) Mean annual carbon emissions from fires during 1997 to 2001 (g C m^{-2} $year^{-1}$).

Table 1. Fire emissions from the forward biogeochemical modeling and inversion approaches.

Region	Forward biogeochemical modeling					Inversion-constrained anomalies						
	Fire emissions		Emission factor (g species per kg dry matter*)				Yearly anomaly (Pg C yr^{-1})					
	1997–2001 average (Pg C yr^{-1})	El Niño anomaly (Pg C)†	CO_2	CO	CH_4	Inversion scalar‡	1997	1998	1999	2000	2001	El Niño anomaly (Pg C)†§
Central and northern South America‖	0.27	0.24	1596 ± 97	84 ± 22	4.2 ± 1.4	1.86 ± 0.83	−0.09	0.41	−0.16	−0.11	−0.04	0.45 ± 0.31
Southern South America‖	0.80	0.34	1598 ± 96	82 ± 21	4.1 ± 1.4	0.69 ± 0.33	0.09	0.13	0.08	−0.21	−0.08	0.23 ± 0.16
Northern Africa‖	0.80	−0.12	1608 ± 96	70 ± 21	2.8 ± 1.0	1.13 ± 1.12	0.06	0.08	−0.06	0.07	−0.15	−0.14 ± 0.15
Southern Africa‖	1.02	0.25	1611 ± 96	67 ± 20	2.5 ± 1.0	0.16 ± 0.47	−0.03	0.04	−0.01	−0.01	0.00	0.04 ± 0.12
Southeast Asia¶	0.37	0.34	1592 ± 93	90 ± 21	5.1 ± 1.6	3.90 ± 0.81	0.71	0.26	−0.14	−0.60	−0.23	1.34 ± 0.67
Boreal (regions north of 38°N)	0.14	0.14	1577 ± 125	100 ± 33	4.3 ± 1.7	1.62 ± 0.12	−0.13	0.32	−0.08	−0.01	−0.09	0.23 ± 0.12
Other#	0.13	−0.03	1605 ± 101	73 ± 23	2.7 ± 1.1	1.13 ± 1.67	−0.01	−0.06	0.04	0.01	0.04	−0.03 ± 0.04
Global	3.53	1.17	1603 ± 97	76 ± 21	3.4 ± 1.2	–	0.59	1.17	−0.34	−0.87	−0.56	2.13 ± 0.79

*The emissions factors and standard deviations (*24*) represent the contribution of each biome (tropical forest, savanna and grassland, and extratropical forest) to total emissions over the 1997 to 2001 period. †The El Niño anomaly period was defined as August 1997 through September 1998. ‡Reported uncertainties represent 95% confidence limits. §Reported uncertainties represent 95% confidence limits and were obtained by combining, in quadrature, uncertainties from the CO inversion with uncertainties from the CO emissions factor. ‖Northern and southern continental regions were divided at the equator. ¶Southeast Asia defined here as Asia east of Pakistan and south of China. #"Other" regions included Australia, the United States and Europe south of 38°N, and Asia south of 38°N (but not including Southeast Asia).

of the variability in CO as predicted by our inversion over the 1997 to 2001 period (table S2). Low interannual variability was required from fire emissions from northern and southern Africa and from the combination of regions defined as "Other" in Table 1.

Converting these CO emissions anomalies to total carbon emissions anomalies by using published emissions factors (*23*), we found that Southeast Asia accounted for ~60% of the carbon emissions during the El Niño period (Table 1), with other important and previously underestimated contributions from Central America and northern South America (20%), boreal forests (10%), and southern South America (10%). The emissions anomaly from Central and northern South America comprised about a third of that from Southeast Asia and influenced atmospheric trace gas anomalies in early 1998 at flask stations in low latitudes of the Northern Hemisphere. Globally, the carbon emissions anomaly from fires during the El Niño period was 2.13 ± 0.79 Pg C. Year by year, carbon emissions from fires were highest in 1998, and lowest in 2000, with a difference of more than 2 Pg C year^{-1} between these two extreme fire years.

Figure 3 shows the atmospheric growth rate anomalies of CO, CO_2, and CH_4. The lack of agreement between the forward model and the observed CO growth rate anomaly in 1997 reflects the underestimation in the CASA model of the CO emissions anomaly arising from fires in Southeast Asia at that time (Fig. 3A and Table 1). As expected, the CO growth rate anomaly calculated from the inversion-optimized fluxes closely matched the observed atmospheric growth rate anomaly. Nevertheless, the close match between the observed and fitted values is marked, given that only seven parameters (one scaling factor for each region over the full 60-month period) were adjusted in the inversion (Fig. 3 and fig. S1). For CO_2 and CH_4, the contribution of fire emissions to the observed atmospheric growth rates was calculated independently of trace gas observations of these species; our estimate only depended on the optimal fluxes of CO derived from our CO inversion and the emission factors connecting these other trace gases to CO (*24*) as reported in Table 1.

The CO_2 growth rate anomaly caused by fire emissions (as obtained from the inversion) had the same general shape as the observed CO_2 growth rate anomaly but was smaller in magnitude (accounting for 66 ± 24% of the observed growth rate during the El Niño period). Thus, in our study, fires were not able to explain the entire observed CO_2 anomaly, and other processes, such as an offset between respiration and photosynthesis in response to drought stress, must account for the remainder. Although evidence from multiple spatial scales shows that terrestrial net primary production decreases during El Niño events (*9*, *10*), it remains highly uncertain whether heterotrophic respiration decreases in parallel or to a greater or lesser extent (supporting online text).

The CH_4 anomaly predicted by our approach was higher than observed in the latter half of 1997 (Fig. 3C). The dry conditions in late 1997 that triggered increases in fire activity may have also reduced anaerobic conditions in tropical soils, lowering CH_4 emissions. This response could have caused our fire-driven model to overestimate the growth rate of CH_4 during this period. Although a previous study has identified wetlands as the primary source of the anomaly in the northern extratropics (*5*), our analysis suggests that almost all of the CH_4 anomalies observed during 1997 and 1998 in this region can be attributed to fires (fig. S2).

There are several reasons why our estimate of the global carbon emissions anomaly from fire during the 1997 to 1998 El Niño is likely to represent an upper bound, including a lack of an explicit treatment of peat lands in our forward model (*13*), attribution of fluxes to boreal regions (that lead to larger surface concentration anomalies per unit of emitted trace gas), and a linear approximation of OH chemistry in the inversion [e.g., (*27*)]. Each of these processes is discussed in greater detail in (*23*). Other major uncertainties in our approach included the use of a repeating set of atmospheric winds from 2000 in our atmospheric chemistry model and our methodology for deriving burned area from

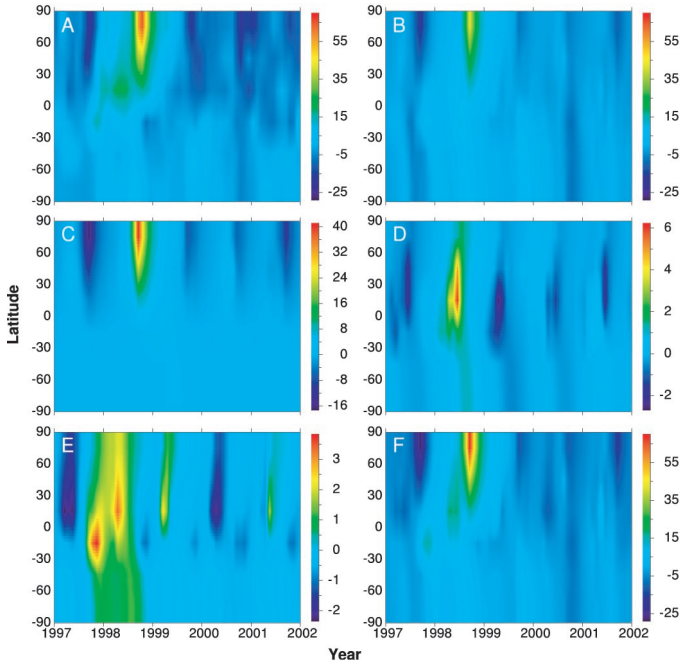

Fig. 2. Global CO concentration anomalies for 1997 to 2001 (in ppb). (**A**) Observed anomalies from the NOAA-CMDL flask network. (**B**) Simulated CO anomalies obtained from our biogeochemical model and the GEOS-CHEM atmospheric chemistry model. (**C**) Model-simulated CO anomalies caused solely by fire emissions from the boreal forests of North America and Eurasia. (**D**) Same as (C) but for Central America and northern South America (north of the equator). (**E**) Same as (C) but for Southeast Asia. Note that the color scaling in (C) to (E) was individually adjusted to highlight the space-pattern of CO anomalies unique to each region. (**F**) The distribution of CO anomalies obtained from our inversion. The inversion-derived estimate shown in (F) represents a linear combination of the CO anomaly patterns obtained from our forward model for the seven regions listed in Table 1 [including those shown in (C) to (E)]. At each station, we removed a mean seasonal cycle derived from CO concentrations over the 1997 to 2001 period.

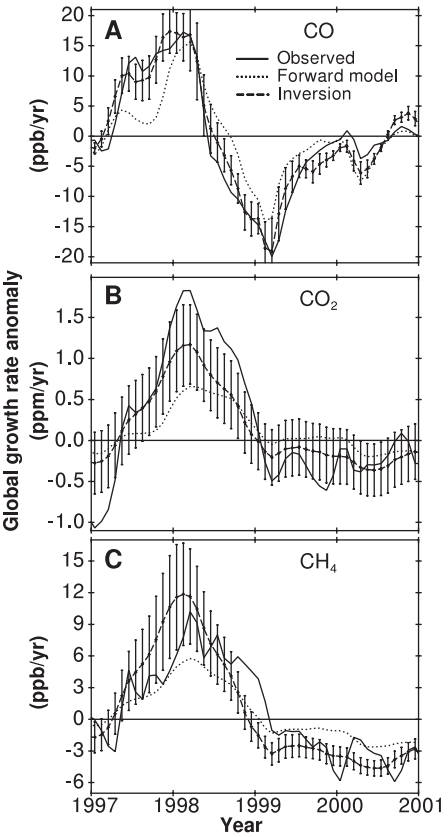

Fig. 3. Atmospheric CO (**A**), CO_2 (**B**), and CH_4 (**C**) growth rate anomalies from the NOAA/CMDL network (solid lines). Fire contributions to the observed growth rates from the forward model are represented with a dotted line, and inversion model estimates are represented with a dashed line (with 1 σ error bars). The error estimates were obtained by combining the errors (in quadrature) from the emission factors reported in Table 1 with the uncertainties on the scalars obtained from the least squares inversion.

the satellite data, although time-invariant biases in burned area or emissions were corrected for by the inversion. We have chosen to limit our inversion to estimating seven parameters on the basis of the availability of a global, multiyear satellite data set of fire activity and the relative sparseness of trace gas measurements used in the inversion. Potential aggregation errors in time and space (*30*, *31*) associated with this choice are other sources of uncertainty in our approach.

We have provided a set of constraints on the distribution of global fire emissions by combining satellite measurements with atmospheric data. Without the use of satellite data, it is difficult to attribute trace gas sources to different tropical regions with standard inversion techniques (*32*). Our analysis reaffirmed the importance of fires in Southeast Asia but also identified fires from other regions as substantial contributors to CO_2 and CH_4 anomalies during 1997 to 2001. This work suggests that the variability and intensity of El Niño may be one of the most critical components of climate regulating future carbon loss. It also indicates that regions that have long served as carbon sinks may suddenly become sources (*33*). An important next step is to develop a means of separating fire emissions from land clearing, pasture maintenance, agricultural waste burning, and forest and savanna fires by using new high-resolution satellite data.

References and Notes

1. C. D. Keeling *et al.*, in *Aspects of Climate Variability in the Pacific and the Western Americas*, D. H. Peterson, Ed. *Geophys. Monogr. 55* (American Geophysical Union, Washington, DC, 1989), pp. 165–236.
2. T. J. Conway *et al.*, *J. Geophys. Res.* **99**, 22831 (1994).
3. M. Battle *et al.*, *Science* **287**, 2467 (2000).
4. E. J. Dlugokencky, L. P. Steele, P. M. Lang, K. A. Masarie, *J. Geophys. Res.* **99**, 17021 (1994).
5. E. J. Dlugokencky, B. P. Walter, K. A. Masarie, P. M. Lang, E. S. Kasischke, *Geophys. Res. Lett.* **28**, 499 (2001).
6. J. T. Houghton *et al.*, Eds., *Climate Change 2001: The Scientific Basis* (Cambridge University Press, Cambridge, 2001).
7. P. Bousquet *et al.*, *Science* **290**, 1342 (2000).
8. K. Lee, R. Wanninkhof, T. Takahashi, S. C. Doney, R. A. Feely, *Nature* **396**, 155 (1998).
9. C. D. Jones, M. Collins, P. M. Cox, S. A. Spall, *J. Clim.* **14**, 4113 (2001).
10. R. R. Nemani *et al.*, *Science* **300**, 1560 (2003).
11. D. A. Clark, S. C. Piper, C. D. Keeling, D. B. Clark, *Proc. Natl. Acad. Sci. U.S.A.* **100**, 5852 (2003).
12. R. L. Langenfelds *et al.*, *Global Biogeochem. Cycles* **16**, 1048 (2002).
13. S. E. Page *et al.*, *Nature* **420**, 61 (2002).
14. J. G. Goldammer, R. W. Mutch, Eds., "Global forest fire assessment 1990–2000" (FAO Forestry Department, 2001).
15. D. C. Nepstad *et al.*, *Nature* **398**, 505 (1999).
16. T. Phulpin, F. Lavenu, M. F. Bellan, B. Mougenot, F. Blasco, *Int. J. Remote Sens.* **23**, 1943 (2002).
17. E. S. Kasischke, L. P. Bruhwiler, *J. Geophys. Res.* **107**, 8146 (2002).
18. S. G. Conard *et al.*, *Climatic Change* **55**, 197 (2002).
19. D. Schimel, D. Baker, *Nature* **420**, 29 (2002).
20. C. Rödenbeck, S. Houweling, M. Gloor, M. Heimann, *Atm. Chem. Phys. Discuss.* **3**, 2575 (2003).
21. Southern Oscillation Index obtained from the Australian Bureau of Meteorology, available online at www.bom.gov.au/climate/current/soihtm1.shtml.
22. G. R. van der Werf, J. T. Randerson, G. J. Collatz, L. Giglio, *Global Change Biol.* **9**, 547 (2003).
23. Materials and methods are available as supporting material on *Science* Online.
24. M. O. Andreae, P. Merlet, *Global Biogeochem. Cycles* **15**, 955 (2001).
25. CASA also predicted variations in Net Ecosystem Production fluxes over this period using Normalized Difference Vegetation Index and climate time series as inputs; however, we did not use these fluxes in our analysis reported here.
26. I. Bey *et al.*, *J. Geophys. Res.* **106**, 23073 (2001).
27. P. C. Novelli *et al.*, *J. Geophys. Res.* **108**, 4464 (2003).
28. P. Bergamaschi, R. Hein, M. Heimann, P. J. Crutzen, *J. Geophys. Res.* **105**, 1909 (2000).
29. S. Curtis, R. Adler, G. Huffman, E. Nelkin, D. Bolvin, *Int. J. Climatol.* **21**, 961 (2001).
30. T. Kaminski, P. J. Rayner, M. Heimann, I. G. Enting, *J. Geophys. Res.* **106**, 4703 (2001).
31. P. Peylin, P. Bousquet, P. Ciais, *Science* **294**, 5541 (2001).
32. M. Gloor, S. M. Fan, S. Pacala, J. Sarmiento, *Global Biogeochem. Cycles* **14**, 407 (2000).
33. C. Körner, *Science* **300**, 1242 (2003).

34. This work was funded by NASA EOS-IDS grants NAG5-9462 (J.T.R.), NAG5-9440 (E.S.K.), and NAG5-9605 (P.S.K.). We thank T. Schneider for advice on the inversion; P. Novelli, T. Conway, P. Tans, and E. Dlugokencky from the NOAA Climate Monitoring and Diagnostics Laboratory for providing the trace gas observations; and K. Treseder for comments on an earlier draft.

Supporting Online Material

www.sciencemag.org/cgi/content/full/303/5654/73/DC1
Materials and Methods
SOM Text
Figs. S1 and S2
Tables S1 and S2
References

25 August 2003; accepted 19 November 2003

Crystal Structure of Biotin Synthase, an *S*-Adenosylmethionine–Dependent Radical Enzyme

Frederick Berkovitch,[1] Yvain Nicolet,[1] Jason T. Wan,[2] Joseph T. Jarrett,[2] Catherine L. Drennan[1]*

The crystal structure of biotin synthase from *Escherichia coli* in complex with *S*-adenosyl-L-methionine and dethiobiotin has been determined to 3.4 angstrom resolution. This structure addresses how "AdoMet radical" or "radical SAM" enzymes use Fe_4S_4 clusters and *S*-adenosyl-L-methionine to generate organic radicals. Biotin synthase catalyzes the radical-mediated insertion of sulfur into dethiobiotin to form biotin. The structure places the substrates between the Fe_4S_4 cluster, essential for radical generation, and the Fe_2S_2 cluster, postulated to be the source of sulfur, with both clusters in unprecedented coordination environments.

Biotin synthase (BioB) catalyzes the final step in the biotin biosynthetic pathway, the conversion of dethiobiotin (DTB) to biotin. This remarkable reaction uses organic radical chemistry for the insertion of a sulfur atom between nonactivated carbons C6 and C9 of DTB (Scheme 1). BioB is a member of the "AdoMet radical" or "radical SAM" superfamily, which is characterized by the presence of a conserved CxxxCxxC sequence motif (C, Cys; x, any amino acid) that coordinates an essential Fe_4S_4 cluster, as well as by the use of *S*-adenosyl-L-methionine (AdoMet or SAM) for radical generation (*1*–*3*). AdoMet radical enzymes act on a wide variety of biomolecules. For example, BioB and lipoyl–acyl carrier protein synthase (LipA) are involved in vitamin biosynthesis; lysine 2,3-aminomutase (LAM) facilitates the fermentation of lysine; class III ribonucleotide reductase (RNR) activase and pyruvate formate-lyase (PFL) activase catalyze the formation of glycyl radicals in their respective target proteins; and spore photoproduct lyase repairs ultraviolet light–induced DNA damage.

AdoMet has been referred to as the "poor man's adenosylcobalamin" (*4*) because of the ability of both cofactors to generate a highly reactive 5′-deoxyadenosyl radical (5′-dA·), formed through homolytic cleavage of a C-Co bond in the case of adenosylcobalamin (AdoCbl) and through reductive cleavage of a C-S bond in the case of AdoMet (*5*). In AdoMet radical enzymes, the formation of 5′-dA· requires the addition of one electron, provided in *E. coli* by reduced flavodoxin and transferred first into an Fe_4S_4 cluster and then into AdoMet (*3*). In the reaction catalyzed by BioB, there is general agreement that 5′-dA· generated from AdoMet oxidizes DTB (*6*), but the number and types of FeS clusters and of other cofactors involved in the reaction have been a subject of controversy (*7*–*14*). Protein preparation–dependent cofactor differences have led to two mechanistic proposals for the method of S insertion in BioB. One proposal involves the use of an Fe_2S_2 cluster

[1]Department of Chemistry, Massachusetts Institute of Technology, Cambridge, MA 02139, USA. [2]Johnson Research Foundation and Department of Biochemistry and Biophysics, University of Pennsylvania, Philadelphia, PA 19104, USA.

*To whom correspondence should be addressed. E-mail: cdrennan@mit.edu